Recent advances in understanding the capacitive storage in microporous carbons

Barbara Daffos, Pierre-Louis Taberna, Yury Gogotsi, Patrice Simon

Fuel Cells

Recent advances in understanding the capacitive storage in microporous carbons

Journal:	*Fuel Cells*
Manuscript ID:	fuce.200900192.R3
Wiley - Manuscript type:	Review
Date Submitted by the Author:	29-Jan-2010
Complete List of Authors:	DAFFOS, Barbara; Université Paul Sabatier, CIRIMAT TABERNA, Pierre-Louis; Université Paul Sabatier, CIRIMAT GOGOTSI, Yury; Drexel University, Department of Materials Science and Engineering and A.J. Drexel Nanotechnology Institute SIMON, Patrice; Universté Paul Sabatier, CIRIMAT
Keywords:	Electrical Storage Systems, Electrochemical, Electrochemical Power Sources, Electrochemical Impedance Spectroscopy, Mass Transport

Recent advances in understanding the capacitive storage in microporous carbons

B. Daffos,[1] P.-L. Taberna,[1] Y. Gogotsi[2] and P. Simon[1,*]

[1]*Université de Toulouse, CIRIMAT, UMR-CNRS 5085, 31062 Toulouse Cedex 4, France*
[2] *Department of Materials Science and Engineering and A.J. Drexel Nanotechnology Institute, Drexel University, Philadelphia, PA 19104, USA*
** Corresponding author*

Abstract

This article presents a review of our recent work on capacitance of carbide-derived carbons. Specific capacitance as high as 14 µF/cm² or 160 F/g was achieved using carbide-derived carbons with tailored subnanometer pore size, which is significantly higher than 6 µF/cm² or 100 F/g) for conventional activated carbons. Such high capacitance was obtained in several types of organic electrolytes with or without solvent. A maximum is obtained for the carbons with the mean pore size close to the bare ion size, ruling out the traditional point of view that mesoporosity is highly required for maximum capacitance. Surprisingly, carbons with subnanometer porosity exhibit high capacitance retention, since only a 10% loss is measured when 6 A/g discharge is drawn. These findings show the importance of fitting the ion size with the mean pore size. The double layer theory falls short to explain such charge storage mechanisms at the nanometer scale, thus atomistic modeling is required to find out an alternative charge storage model.

1. Introduction

Electrical Double Layer Capacitors (EDLCs), also known as supercapacitors, are one of the most promising electrochemical energy storage devices for high power delivery or energy harvesting applications (*1-3*). EDLCs charge storage mechanism is electrostatic by nature, and requires storage of opposite charges at the two electrodes, properly balanced by the ions from the electrolyte. This is achieved through the reversible adsorption of ions from an electrolyte onto high surface area carbons.

Differentiating from batteries or pseudocapacitors (*1, 3*), there is no redox reaction involved in the charge storage mechanism and the charge is stored at the surface of the carbon materials. Accordingly, it can be quickly released or captured and this explains the high power capability of EDLCs. As a drawback, the amount of charge stored at the surface is limited and the energy density of the EDLCs will always be about an order of magnitude lower than that of batteries. EDLCs are already used in many commercial applications such as power electronics, aircrafts, cranes, elevators, tramways and others (*3*). One of the most promising applications are the Hybrid Vehicles (HVs) in combination with Internal Combustion Engines, and the Electric Vehicles (HEVs) where EDLCs could be combined with a battery pack for braking energy recovery or short-time acceleration power. For a fuel-cell powered HEV, the use of EDLCs would be of great interest for power delivery during the first seconds the fuel cell needs to reach operational state.

Today, the energy density achieved by commercial products (about 5 $Wh.kg^{-1}$) limits their use to few seconds of charge/discharge, which is sufficient for energy harvesting (recovery of potential energy in cranes and elevators, braking energy in tramways and HEVs or mechanical energy coupled with MEMS) (*3*). However, increase of the operation time up to 10 s or more would definitely secure a place for supercapacitors at the forefront of the energy

storage harvesting devices. Therefore improving the energy density of supercapacitors would enable many new applications.

Being proportional to the voltage square, both power and energy are increased when the cell voltage is increased as shown in equations (1) and (2) below:

$$E = \frac{1}{2} C \times V^2 \quad (1)$$

$$P = \frac{V^2}{4R} \quad (2)$$

where V is the cell voltage (V), E is the energy (J), C is the capacitance (F), P is the power (W) and R is the series resistance (Ω).

Therefore, much effort focused on the increase of the operating voltage of supercapacitors by designing new electrolytes (*4*)(*5*). One strategy today is the use of ionic liquids as electrolytes (*6*)(*7*)(*8*)(*9*), which can ensure a high cell voltage (up to 4V), despite a low ionic conductivity.

Combining a faradic electrode with an EDLC electrode is another way to improve the energy density. Such systems, named Hybrid Capacitors, reach high energy densities of more than 15 $Wh.kg^{-1}$ for the Li-ion capacitor operating in organic electrolyte with a pre-lithiated graphite negative electrode (*10*). The combination of a negative carbon electrode to a MnO_2 (*11*)(*12*)(*13*)(*14*), NiOOH (*15*)(*16*) or PbO_2 (*17*)(*18*) positive electrodes leads to high power hybrid systems operating in aqueous electrolytes.

However, whatever hybrid systems are being considered, they still suffer from the drawbacks linked to the faradic electrode, which are a limited cyclability for high depth of discharge (> 70%) or high rate of charge (*19*). Another route to increase the energy density of

supercapacitors, is to keep the symmetric EDLC carbon/carbon system and increase the capacitance of these porous carbons. This solution may appear as more complex, since there is less flexibility on the choice of the materials, but the supercapacitor cyclability, power performance and low temperature behaviors are preserved (*3*). In this paper, we will try to give an update on the most recent work relating to the design of microporous carbons for EDLC applications.

2. Discussion

2.1 Capacitance vs pore size in organic electrolytes

EDLCs are electrochemical capacitors that store the charge electrostatically using reversible adsorption of ions of the electrolyte onto active materials that are electrochemically stable and have high accessible SSA. Charge separation occurs on polarization at the electrode–electrolyte interface, producing what Helmholtz (21) described in 1853 as the double layer capacitance (20,22) *C*

$$C = \frac{\varepsilon A}{d} \quad , \quad (3)$$

where ε is the electrolyte dielectric constant, *A* - the surface area accessible to ions and *d* - the distance between the centre of the ion and the carbon surface. EDLCs use high specific surface area (SSA) carbons to increase the total available surface area for ion adsorption. Such carbons are traditionally obtained from carbon-rich organic precursors by heat treatment in inert atmosphere (carbonisation process). High surface area is achieved through what is called the "activation" consisting in a partial, controlled oxidation of the carbon precursor (*23*). SSA as high as 1,500 – 2,600 $m^2.g^{-1}$ can be achieved by activation.

The specific capacitance of carbons expressed in Farads per gram of carbon ($F.g^{-1}$) shows a linear dependence on surface area up to 1500 $m^2.g^{-1}$, but tends rapidly to plateau when SSA is further increased (*24*). As a consequence, the way in which the surface is developed has a great impact on the value of specific capacitance achieved. One of the key issues in designing nanostructured carbons for EDLC applications is then the understanding of the relationship between the electrolyte ion size and the carbon pore size (*25*)(*26*). Because of the mean size of the solvated ions in non-aqueous electrolytes (about 1nm) (*27*), a mean carbon pore size of about 2-3 nm was thought to be the best compromise to reach high capacitance values. Indeed, such pore size was large enough to host adsorbed ions on both sides of the carbon pore walls but small enough to minimize the voids and maximize the energy density (Fig. 1). However, all attempts to prepare carbons using standard activation or template-based synthesis failed to significantly increase the carbon capacitance (*3*). At the same time, some authors mentioned that surprisingly high capacitance could be obtained with microporous carbons, and this suggested that even the small micropores (size less than 2 nm) could contribute to the charge storage (*26*)(*28*)(*29*).

Charge storage in pores smaller than the size of solvated ions of the electrolyte has been recently demonstrated by using Carbide Derived Carbons (CDCs) (*30*). CDCs were obtained by chlorination of a metal carbide (TiC in our case) according to

$$TiC + 2Cl_2 \rightarrow TiCl_4 + C \qquad (4)$$

Using this synthesis process, it is possible to prepare carbons with a fine-tuned and a narrow pore size distribution, which is definitely not possible through the standard activation process (*23*). CDCs with controlled pore size from 0.6 to 1 nm were prepared and electrochemically tested in a 1.5M NEt_4BF_4 in acetonitrile electrolyte.

Figure 1 shows the change of the normalized capacitance vs the carbon pore size; normalized capacitance ($\mu F.cm^{-2}$) was obtained by dividing the gravimetric capacitance by the SSA. Some data from the literature obtained with mesoporous carbons reported in Figure 1 follows the expected traditional behavior: when the carbon pore size decreases in the mesoporous range (down to 2 nm), the normalized capacitance decreases. However, the results obtained with the CDCs in the 0.6 – 1 nm pore range show a sharp capacitance increase following a power law dependence with r_{pore}^{-1}. This was the first demonstration of the anomalous capacitance increase observed with microporous carbons with controlled, narrow pore size distribution. Such micropores, smaller than the size of the solvated NEt_4^+ and BF_4^- ions in acetonitrile (*27, 30*), were thus accessible to the ions of the electrolyte. The proposed hypothesis was that these narrow pores were accessible thanks to a partial desolvation of the ions. A smaller approaching distance (d) of the ion to the carbon surface was responsible for the capacitance increase according to equation (3).

Several recent studies confirmed these results. Kaneko's group observed with carbon nano-horns that ions were able to pass through gates smaller than the size of the solvated ions in propylene carbonate-based electrolytes (*27*). Meunier's group proposed a mathematical fit of the anomalous capacitance increase in these micropores based on the Electrical Wire-in-Cylinder model (EWC) capacitance equation (*31, 32*). Thanks to this model, it was possible to calculate an average size of the ions inside the pores, which was found to be smaller than the bare ion size.

Surprisingly, the power capability of laboratory EDLC devices assembled with CDCs powders was not deeply affected by the use of microporous carbons. Figure 2a shows a Nyquist plot for different CDC samples (0.72 – 1.1 nm). AC Series resistance (measured at

high frequency) as low as 0.5 Ohm.cm² was obtained in 1.5 M NEt_4BF_4 in an acetonitrile electrolyte. At low frequencies, where the ionic resistance of the electrolyte inside the porous network can be seen, the DC resistances were in the range of 2-3 Ohm.cm², i.e. in the same range as for activated carbon-based electrodes *(33)*. The capacitance increase using these microporous carbons was not achieved at the expense of the power performance since these series resistance values are similar to that of standard activated carbons (*33*). Figure 2b shows the capacitance change vs the current density. The capacitance retention was found to be very good, with only a 10% loss for the best sample (0.72 nm) when the current was increased up to 6 $A.g^{-1}$. The power capability of the CDCs was very good when the pore size was well adapted to the ion size, between 0.72 and 0.76 nm. Thus, it is possible to reach high energy and high power density with sub-nanometer microporous carbons.

Using the Cavity Micro Electrode technique (CME) developed by Cachet-Vivier et al. (*34*), we have studied the electrochemical behavior of the CDCs in NEt_4BF_4 in acetonitrile electrolyte (*35*). The CME allowed the recording of electrochemical behavior of active material eliminating effects of separators, current collectors and other device components. Figure 3 shows the CVs of four CDC samples recorded at 100 $mV.s^{-1}$ in 1.5 M NEt_4BF_4 in AN electrolyte between–1.3 V/Ref. and +1 V/Ref. All the plots were normalized to the maximum capacitive current at 1 V/ref.. The capacitive behavior originates from the NEt_4^+ cation adsorption negative of the OCV, which was measured close to 0 V/Ref for all samples. For potential higher than OCV, the BF_4^- anions adsorption can be seen. In this potential range (potentials higher than OCV), the CVs are rectangular-shaped - typical for pure double-layer capacitive behavior. When the potential scan is reversed at 1 V/Ref to negative, only slight changes in the CVs can be observed above the OCV. This potential range corresponds to the discharge of the positive electrode, where anions are removed from the porous carbons. When

the potential scan was negative of the OCV (0 V/Ref), the rectangular shape of the CV was lost for all samples except the one with the largest pore size (1 nm). The smaller the pore size (the lower the synthesis temperature), the more distorted the CVs. This shift from purely capacitive behavior is also present when the potential scan rate is reversed at -1.3 V/Ref to positive values. These distortions of CVs were also reported by Salitra et al. (*26*) using a conventional 3-electrode cell with an activated carbon cloth as the active material. They were linked with the limitation in the pore accessibility because of the well-known "sieving effect" (*26, 36*) hampering the ion transport inside the small, narrow pores.

From these measurements, it was deduced that anion adsorptions could occur without any limitation even for pore size of 0.68 nm (rectangular shape of the CVs), that meant that the effective anion size seen by the carbon during the adsorption was ≤ 0.68 nm. In the same way, the effective size of the adsorbed cation in AN during double layer charging/discharging can be estimated between 0.76 nm and 1 nm, since CV distortions were observed for pore size less than 0.76 nm. Comparing these effective ion size to the solvated ion size (1.3 nm and 1.16 nm for the cation and the anion respectively), it appears obvious that the ions need to be, at least, partially desolvated to enter the micropores smaller than 1 nm, thus confirming the previous results. Recent results reported by Mysyk et al. (*37*) confirmed this sieving effect. However, in this recent paper, only 2-electrode measurements were made and it was not possible to distinguish between anion and cation contributions to the capacitive process.

2.2 Capacitance vs pore size in solvent-free electrolytes

In a solvent-based electrolyte, the determination of the exact solvation shell is sometimes difficult, depending if one considers the first, second or subsequent solvation sphere. The next step has thus been to try to get free from the ion solvation shell, by using an ionic liquid

electrolyte. The electrochemical characterization of CDC electrodes was conducted at 60°C in Ethyl-MethylImmidazolium-TriFluoro-methane-SulfonylImide ionic liquid (EMI-TFSI), according to two main criteria (*38*). First, the ionic conductivity of the EMI-TFSI neat electrolyte at 60°C is about 15 $mS.cm^{-1}$ which allows the ohmic drop to remain at a reasonable value during electrochemical measurements. Additionally, the ion sizes were calculated as 0.79 nm and 0.76 nm respectively for TFSI and EMI ions, meaning that ion sizes were i) very close were and ii) in the range of the CDC pore size (*38*). Figure 4 shows the change of the gravimetric capacitance (a) and normalized capacitance (b) vs the carbon pore size for the cell, the positive and the negative electrodes (*38*). The normalized capacitance was obtained by dividing the gravimetric capacitance ($F.g^{-1}$) by the SSA ($m^2.g^{-1}$).

In Figure 4, the electrode specific capacitance ($C'_{electrode}$) is calculated from the weight of the carbon in one electrode (m_{carbon}) according to equation (3):

$$C'_{electrode\ (F.g^{-1})} = \frac{C_{electrode}}{m_{carbon}}$$

The calculated electrode capacitance ($C''_{electrode}$) was calculated from the 2-electrode cell capacitance C_{cell} according to equation (4):

$$C''_{electrode(F.g^{-1})} = \frac{2 \times C_{cell}}{m_{carbon}}$$

From Figures 4a and 4b, it can be seen that positive, negative and cell capacitance show a maximum at the same pore size. This is consistent with the similar ion sizes observed for the EMI^+ and $TFSI^-$. More surprising is that the maximum capacitance was obtained for pore size close to the ion size, 0.72 nm. These results rules out the way charge storage is traditionally described in EDLC materials, with ions adsorbed on both pore walls: carbon pore size is here

in the same range as the ion size and there is no space available for more than one ion per pore. However, the maximum capacitance at 0.72 nm agrees well with the ion size, taking into account the asymmetry of the ions and accuracy of pore size measurements. At this point, pore size is perfectly adapted to the ion size and ion adsorption is achieved in an efficient way. Both, larger and smaller pores show a significant drop in capacitance. When pore size is increased, average distance between pore wall and the centre of the ion (d) is increased and then the capacitance for pores larger than around 0.72 nm decreases according to equation (3). For smaller pore size, the steric effect limit the ion accessibility and the capacitance is decreased.

Additionally, a commercial microporous activated carbon tested in the same conditions gave a capacitance of about 100 $F.g^{-1}$ and 6 $\mu F.cm^{-2}$. When compared to the maximum capacitance values reported in Figure 4, it can be seen that matching the pore size close to the ion size leads to a 60% capacitance increase. There is no evidence of any charge saturation like recently reported (*37, 39*); moreover, the opposite effect was observed. This work suggests a general approach to selecting a porous electrode / electrolyte couple in order to maximize the capacitance, which has been now proved for both, organic salt in a solvent and solvent-free liquid electrolytes. More basic work is needed to understand the mechanism of this capacitance increase. In this aim, modeling of ions and their environment when adsorbed inside these narrow subnanometer pores is needed. As an example, Yang et al. (*40*) recently used the molecular simulation to model the electrical double layer capacitance using carbon nanotubes. These simulations confirmed an increase of the capacitance when decreasing the pore size in the microporous range. Combining in-situ experimental measurements to mathematical modeling will be of great help in the understanding of the mechanism of anomalous capacitance increase when carbon pore size matches the ion size. This will affect

not only the energy storage field (EDLCs) but also other applications where ion transport through membranes is required, such as for water desalination or non channels in cells.

3. Conclusions

The most recent advances in supercapacitor materials include development of nanoporous carbons with the pore size tuned to fit the size of ions of the electrolyte with Ångström accuracy. An improved understanding of charge storage and ion desolvation in sub-nanometer pores has helped to overcome a barrier that has been hampering the progress in the field for several decades. It has also stressed the requirement of matching the active materials with specific electrolytes and the need to use a cathode and anode with different pore sizes, which match the anion/cation size. The very large number of possible active materials and electrolytes requires better theoretical guidance for the design of more powerful and long-lasting EDLCs.

Acknowledgements

Work at Paul Sabatier University was supported by Délégation Générale pour l'Armement. Y.G. thanks the US Department of Energy for financial support. Collaboration between the participating universities was supported by a Partnership University Fund (PUF) grant.

References

1. B. E. Conway, *Electrochemical Supercapacitors: Scientific Fundamentals and Technological Applications* (Kluwer, 1999), pp.
2. R. Kotz, M. Carlen, *Electrochimica Acta* **45**, 2483 (2000).
3. P. Simon, Y. Gogotsi, *Nature Materials* **7**, 845 (Nov, 2008).
4. A. Janes, E. Lust, *Journal Of Electroanalytical Chemistry* **588**, 285 (Mar 15, 2006).
5. P. Staiti, F. Lufrano, *Journal Of The Electrochemical Society* **152**, A617 (2005).
6. M. Armand, F. Endres, D. R. MacFarlane, H. Ohno, B. Scrosati, *Nature Materials* **8**, 621 (Aug, 2009).
7. M. Lazzari, F. Soavi, M. Mastragostino, *Journal Of The Electrochemical Society* **156**, A661 (2009).

8. A. Balducci, F. Soavi, M. Mastragostino, *Applied Physics A-Materials Science & Processing* **82**, 627 (Mar, 2006).
9. C. Arbizzani, S. Beninati, M. Lazzari, F. Soavi, M. Mastragostino, *Journal Of Power Sources* **174**, 648 (Dec 6, 2007).
10. e. a. H. Gualous, *Proceedings of the ESSCAP 2008 conference, Roma, Italy, November 6-8 2008* (2008).
11. C. C. Hu, T. W. Tsou, *Electrochemistry Communications* **4**, 105 (Feb, 2002).
12. Y. K. Zhou, M. Toupin, D. Belanger, T. Brousse, F. Favier, *Journal Of Physics And Chemistry Of Solids* **67**, 1351 (May-Jun, 2006).
13. T. Cottineau , M. Toupin, T. Delahaye, T. Brousse and D. Belanger, Applied Phys. A , Materials Science and processing 82 (2006) 599-606.
14. T. Brousse *et al.*, *Journal Of Power Sources* **173**, 633 (Nov 8, 2007).
15. http://www.esma-cap.com/.
16. http://www.elit-cap.com/, (2008).
17. L. T. Lam *et al.*, *Journal Of Power Sources* **174**, 16 (Nov 22, 2007).
18. P. Perret, T. Brousse, D. Belanger, D. Guay, *Journal Of The Electrochemical Society* **156**, A645 (2009).
19. J. Miller, A. F. Burke, *The Electrochemical Society Interface* **17** (2008) 53.
20. G. Gouy, *Compt. Rend.* **149**, 654 (1910).
21. H. V. Helmholtz, *Ann. Phys.* **29**, 337 (1879).
22. O. Stern, *Z. Elektrochem.* **30**, 508 (1924).
23. A. G. Pandolfo, A. F. Hollenkamp, *Journal Of Power Sources* **157**, 11 (Jun 19, 2006).
24. O. Barbieri, M. Hahn, A. Herzog, R. Kotz, *Carbon* **43**, 1303 (2005).
25. M. Endo *et al.*, *Journal Of The Electrochemical Society* **148**, A910 (2001).
26. G. Salitra, A. Soffer, L. Eliad, Y. Cohen, D. Aurback, *Journal Of The Electrochemical Society* **147**, 2486 (2000).
27. C. M. Yang *et al.*, *Journal Of The American Chemical Society* **129**, 20 (Jan 10, 2007).
28. C. Vix-Guterl *et al.*, *Carbon* **43**, 1293 (May, 2005).
29. A. Janes, L. Permann, P. Nigu, E. Lust, *Surface Science* **560**, 145 (2004).
30. J. Chmiola *et al.*, *Science* **313**, 1760 (2006).
31. J. S. Huang, B. G. Sumpter, V. Meunier, *Chemistry-A European Journal* **14**, 6614 (2008).
32. J. S. Huang, B. G. Sumpter, V. Meunier, *Angewandte Chemie-International Edition* **47**, 520 (2008).
33. C. Portet, P. L. Taberna, P. Simon, C. Laberty-Robert, *Electrochimica Acta* **49**, 905 (Mar 1, 2004).
34. C. Cachet-Vivier, V. Vivier, C. S. Cha, J. Y. Nedelec, L. T. Yu, *Electrochimica Acta* **47**, 181 (Sep 1, 2001).
35. R. Lin, Taberna, P.L., Chmiola, J., Guay, D., Gogotsi, Y. and P. Simon, *Journal Of The Electrochemical Society* **156**, A7 (2009).
36. D. Aurbach *et al.*, *Journal Of The Electrochemical Society* **155**, A745 (2008).
37. R. Mysyk, E. Raymundo-Pinero, F. Beguin, *Electrochemistry Communications* **11**, 554 (Mar, 2009).
38. C. Largeot *et al.*, *Journal Of The American Chemical Society* **130**, 2730 (2008).
39. C. O. Ania, J. Pernak, F. Stefaniak, E. Raymundo-Pinero, F. Beguin, *Carbon* **47**, 3158 (Nov, 2009).
40. L. Yang, B. H. Fishbine, A. Migliori, L. R. Pratt, *Journal Of The American Chemical Society* **131**, 12373 (Sep 2, 2009).

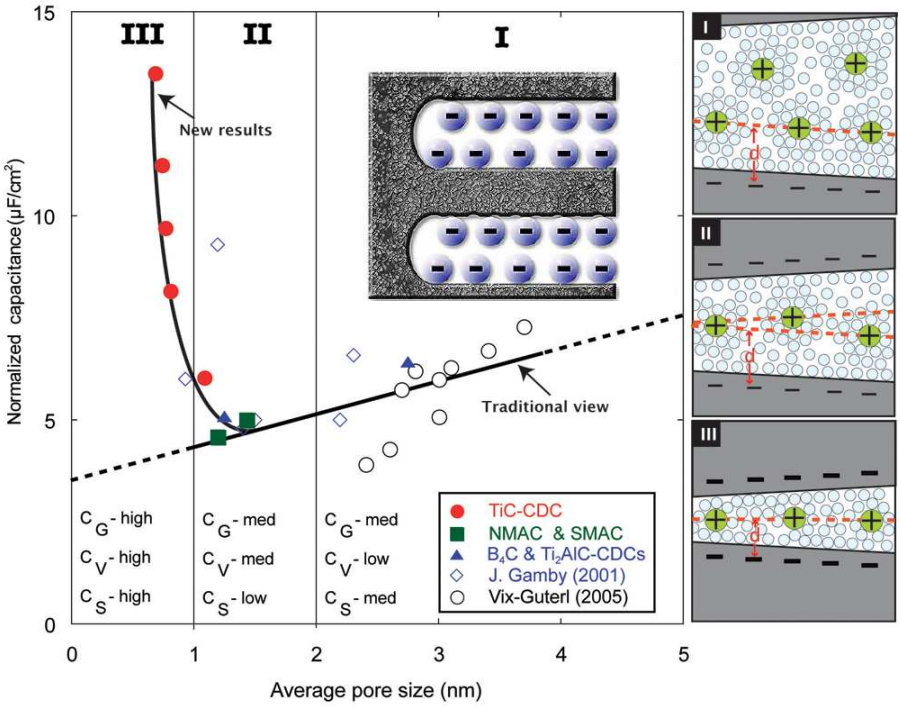

Figure 1:

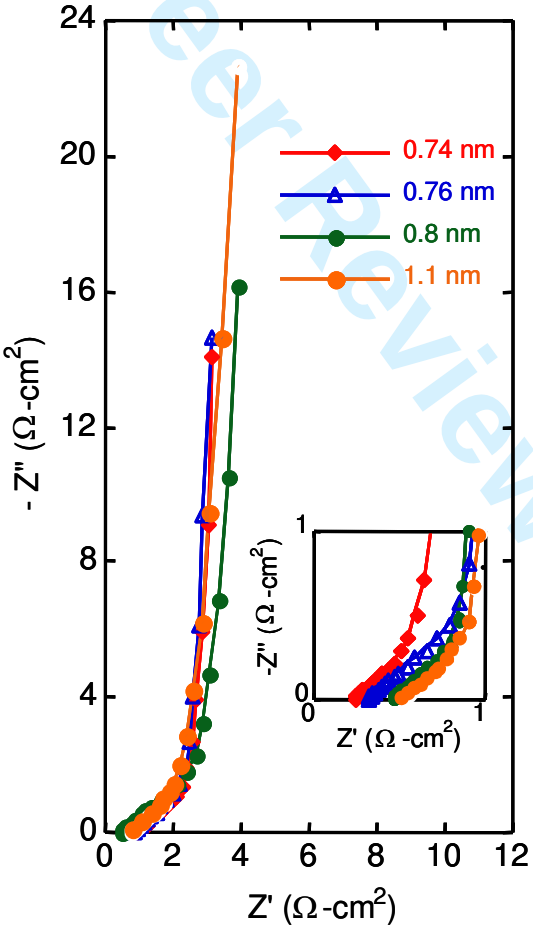

Figure 2a:

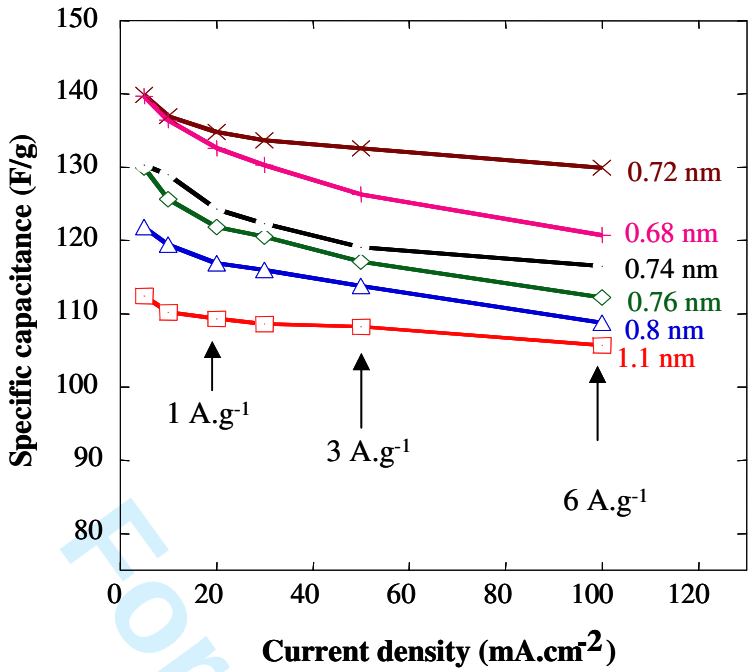

Figure 2b:

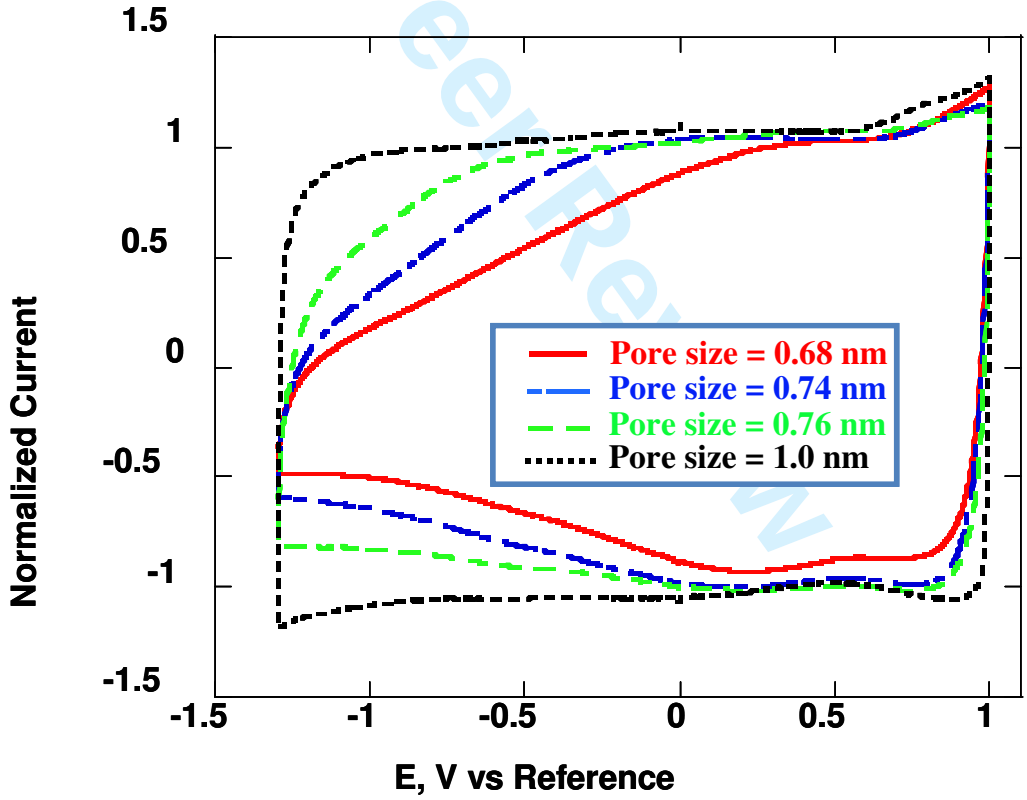

Figure 3:

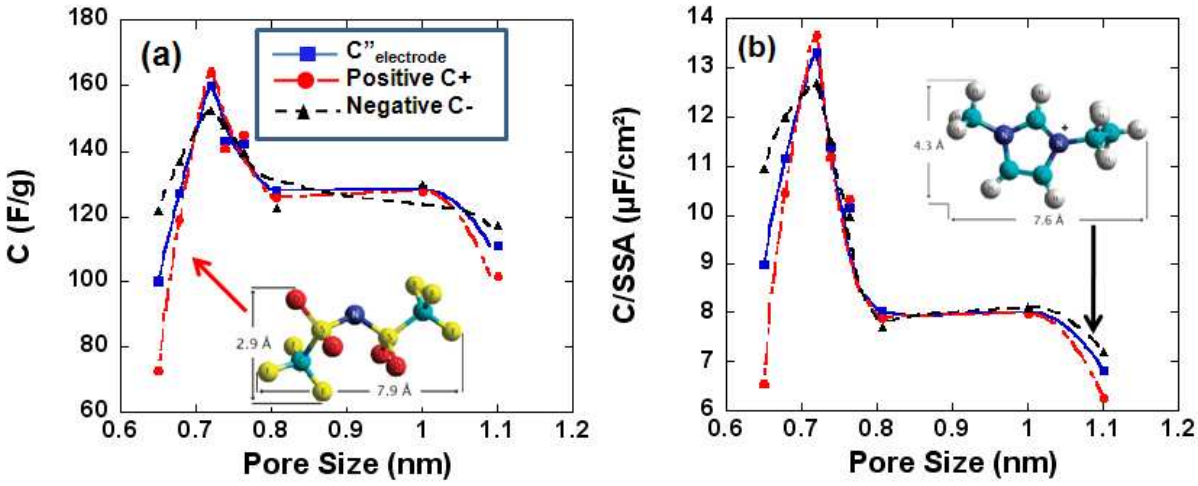

Figure 4:

Figure 1: Change of the normalized capacitance vs the carbon pore size; normalized capacitance ($\mu F.cm^{-2}$) was obtained by dividing the gravimetric capacitance by the SSA; from (30).

Figure 2a: Nyquist plot of supercapacitor cells assembled with CDCs with various pore size in 1.5 M NEt_4BF_4 in AN electrolyte. Frequency range: 10 kHz-10 mHz; bias voltage: 0V.

Figure 2b: Capacitance change vs current density for laboratory cells assembled with CDCs with various pore size.

Figure 3: Cyclic Voltammetries (CVs) of four CDC samples with various pore size (0.68 – 1 nm) recorded at 100 $mV.s^{-1}$ in 1.5 M NEt_4BF_4 in AN electrolyte between –1.3 V/Ref. and +1 V/Ref. (Reference electrode is a silver wire); from (35).

Figure 4: Change of the gravimetric capacitance (a) and normalized capacitance (b) vs the carbon pore size for the cell, the positive and the negative electrodes in EMI,TFSI neat electrolyte at 60°C. Calculated capacitance $C''_{electrode}$ refers to electrode specific capacitance calculated from the overall cell (EDLC) capacitance measured in two-electrode configuration. Capacitance were calculated from galvanostatic charge discharge plots at 10 $mA.cm^{-2}$; from (38).